Effect of plasma waves on the optical properties of conducting superlattices

Marcelo del Castillo-Mussot and W. Luis Mochán
Instituto de Física, Universidad Nacional Autónoma de México, Apartado Postal 20-364, 01000 México, Distrito Federal, Mexico
(Received 20 January 1987)

We calculate the dispersion relation of the electromagnetic normal modes and the reflectance of superlattices made of highly doped semiconductors and of metals, taking into account plasma waves, spatial dispersion, and retardation. We obtain a variety of modes made up of interacting surface and bulk plasmons, which yield a rich structure in the reflectance spectra.

In a recent paper[1] (hereafter referred to as I) a simple transfer-matrix formalism was developed in order to study the effect of plasma waves on the electromagnetic modes and the reflectance of conductor-insulator superlattices. Since conductor-conductor superlattices may be grown from either heavily doped semiconductors[2] or metals,[3] the purpose of this paper is to calculate their optical properties making use of the theory developed in I. Previous efforts to take into account the effects of longitudinal waves in conducting periodic superlattices include the work of Eliasson *et al.*[4] and that of Xue and Tsai.[5] In Ref. 4 a system made up of alternating conducting layers was studied in the nonretarded limit, whereas an electron gas with a sinusoidally modulated equilibrium density was investigated in Ref. 5.

We consider a superlattice made up of a hydrodynamic conductor (A) with plasma frequency ω_A and stiffness constant β_A, in layers of width d_A alternating periodically with a hydrodynamic conductor (B) in layers of width d_B whose plasma frequency is $\omega_B > \omega_A$. At frequencies $\omega < \omega_B$ both longitudinal and transverse waves are evanescent in the B layers. Since the decay distance of longitudinal waves $\delta_B^L \sim \beta_B/\omega_B$ is much smaller than that of transverse waves $\delta_B^T \sim c/\omega_B$, in this paper we will assume $\delta_B^L = 0$. This is equivalent to a stiffness constant $\beta_B = 0$ which in the hydrodynamic model implies the absence of spatial dispersion from the B layers. That is, for frequencies below ω_B we model the nonlocal-nonlocal conducting superlattice by a nonlocal-local one. The appropriateness of this model will be discussed below.

We note that all the formulas of I can be applied to the present system without modification, simply by identifying all quantities in I referring to metallic or insulating layers with the corresponding quantities in this work referring to the hydrodynamic (A) or non-spatially-dispersive (B) layers, respectively. The additional boundary condition (ABC) (Ref. 6) employed in I, namely, continuity of the normal component of the induced current, is consistent[7] with the set of ABC's used in Ref. 4. For convenience we choose a Drude local dielectric function for the B layers and therefore we make the substitution

$$\epsilon_I \to \epsilon_B(\omega) \equiv 1 - \frac{\omega_B^2}{\omega^2 + i\omega/\tau} ,$$

where ϵ_I is the dielectric constant of the insulating layers in I and τ is the electronic relaxation time in the B layers.

In Fig. 1 we show the dispersion relation of the normal modes of a highly doped semiconductor superlattice with $d_A = 100$ Å, $d_B = 5d_A$, carrier densities $n_A = 2.33 \times 10^{17}$ cm^{-3}, $n_B = 2n_A$ and a very large electronic relaxation time. These are the same parameters used in Ref. 4. We used the relations $\omega_\alpha^2 = 4\pi n_\alpha e^2/m$ with $\alpha = A,B$ and

$$\omega_A^2 = \tfrac{3}{5}(V_A^F)^2 = \frac{3\hbar^2}{5m^2}(3\pi^2 n_A)^{2/3} ,$$

where e and m are the electronic charge and mass, respectively, and V_A^F is the Fermi velocity. In order to obtain the dispersion relation ω versus p shown in Fig. 1, we chose a fixed value for the parallel component of the wave vector $Q = 0.5/d_A$, we gave real values to ω and solved Eq. (29) of I analytically for the real and imaginary parts

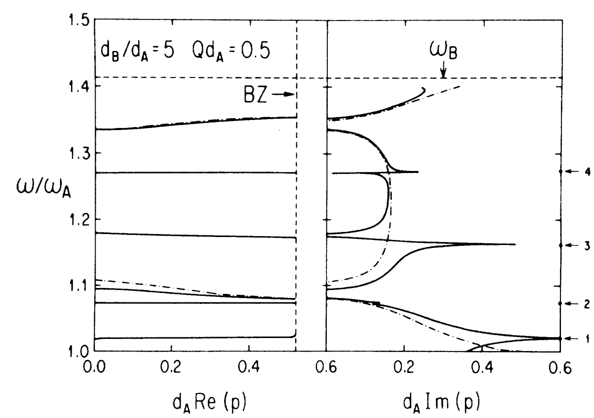

FIG. 1. Nonlocal (solid line) and local (dashed-dotted line) calculation of the dispersion relation ω vs p of a highly-doped semiconductor superlattice with $d_B = 5d_A$ and $Qd_A = 0.5$. The real part of p is shown in the left-hand side panel and its imaginary part in the right-hand side panel. The vertical dashed line indicates the boundary of the Brillouin zone and the single-film resonance plasma frequencies ω_n are indicated by their corresponding integers $n = 1,2,3,4$.

of the Bloch wave vector p, which describes propagation along the axis of the superlattice. The local limit of the dispersion relation is also shown in the same figure. Notice that for the parameters chosen above, retardation is unimportant.

Two propagating modes [finite Re(p) and very small Im(p)] can be seen in the local case around $\omega = 1.1\omega_A$ and $\omega = 1.35\omega_A$. As discussed in I, these two modes are made up of surface plasmons propagating along each interface with wave vector Q and coupled together through the tails of their evanescent fields.[8] These two bands can also be seen in the nonlocal calculation at slightly different frequencies. Besides the coupled surface-plasmon modes, a series of bands, corresponding to coupled guided bulk plasmons in the low-density layers, can be seen near the single-film resonance frequencies ω_n where

$$\omega_n^2 = \omega_A^2 + \beta_A^2 [Q^2 + (n\pi/d_A)^2], \quad n = 1,2,3,\ldots . \tag{1}$$

Comparing our results to those of Ref. 4 we find the same two kinds of modes; those arising from coupled surface plasmons have nearly the same frequency and bandwidth, but those arising from coupled bulk plasmons are displaced towards higher frequencies in our calculation. The reason for this displacement is that the bulk plasmons in Ref. 4 spill over from the A layers, whereas we assumed $\delta_B^L = 0$. The effects of plasmon spillover could be taken into account in Eq. (1) by incrementing d_A by a distance of the order of δ_B^L, which decreases the resonance frequencies by a quantity of order δ_B^L/d_A. The mode corresponding to $n = 1$ has a very large imaginary part in our calculation and it does not appear in Ref. 4, while the mode corresponding to $n = 5$, which appears near $\omega = 1.31\omega_A$ in Ref. 4, is not depicted in our Fig. 1 because it lies too close to ω_B. Recall that near ω_B the penetration length increases, and above ω_B bulk plasmons may propagate in the B layers. The above arguments lead us to note that our results presented in Fig. 1 are qualitatively equivalent to those of Ref. 4, but our results were obtained analytically.

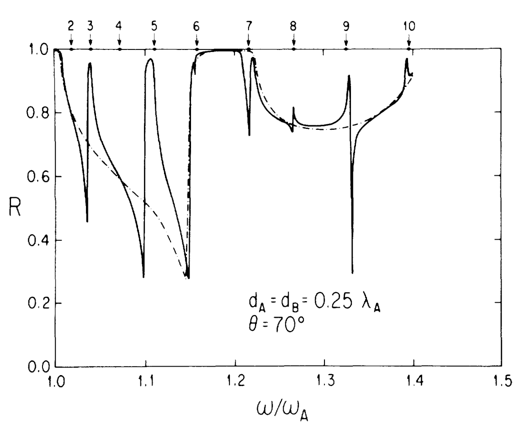

FIG. 2. Nonlocal (solid line) and local (dashed-dotted line) calculation of the reflectance of a semi-infinite metallic superlattice with $d_A = d_B = 0.25\lambda_A$ for an angle of incidence $\theta = 70°$.

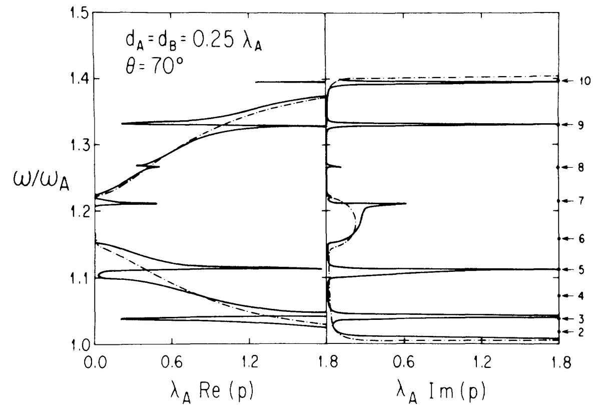

FIG. 3. Dispersion relation ω vs p of a metallic superlattice with $d_A = d_B = 0.25\lambda_A$ for a fixed angle of incidence $\theta = 70°$.

In Fig. 2 we show the reflectance calculated, using Eqs. (31)–(35) of I, for a semi-infinite metal-metal superlattice with $d_A = d_B = 0.25\lambda_A = 0.25c/\omega_A$, $\omega_B = \sqrt{2}\omega_A$, $V_A^F = 0.01c$, and $\tau = 100/\omega_B$, upon whose surface p-polarized light is incident at an angle $\theta = 70°$. We include results of both nonlocal and local calculations. These can be understood by resorting to Fig. 3, where we have plotted ω versus p for a fixed angle of incidence θ instead of a fixed Q. Inclusion of retardation is unavoidable in this case. It can be seen that the reflectance is almost 1.0 at frequencies for which there are no propagating normal modes in the superlattices. Two broad reflection minima are apparent in the local calculation, corresponding to the two surface-plasmon bands shown in the local dispersion relation of Fig. 3.

The nonlocal calculations shown in Figs. 2 and 3 follow grossly the local one, but exhibit a strong oscillating structure around the frequencies ω_n, which is more pronounced for odd n. This structure is due to the resonant coupling between surface plasmons and guided plasmons. The structure at ω_7 lies in the local gap and corresponds to plasmon-mediated propagation. Unlike our present results for conductor-conductor superlattices there is no coupling between surface and bulk plasmons in conductor-insulator superlattices[1] since in them the surface-plasmon bands have a lower frequency than do the bulk plasmons. Another difference is that we found two broad minima in the reflectance originating in the surface-plasmon bands, whereas only one was found in I. The reason for this is that surface plasmons may exist inside the light cone at metal-metal interfaces.

In summary, we have used a simple theory[1] to calculate the optical properties of conductor-conductor superlattices taking into account retardation, the presence of plasma waves, and their coupling to transverse waves. We used a hydrodynamic approach, neglecting the nonlocality of the layers with higher plasma frequency. Thus, our results can only be used for frequencies below the highest plasma frequency, and they are accurate whenever the plasmon spillover from the low-density layers can be neglected. This occurs provided the decay distance of longitudinal waves in the more dense layers is much smaller than any other relevant distance. We have identified electromagnetic bulk modes made up of surface plasmons and of guided bulk plasmons coupled among themselves and with each other. The inclusion of retardation allowed us to calculate their effect on optical reflectivity. There are previous calculations of the reflectivity of conductor-conductor superlattices, such as that of Ref. 5, but to our knowledge, ours is the first such calculation to take into account the coupling of transverse and longitudinal waves.

We acknowledge useful discussions with Rubén G. Barrera. This work was financially supported in part by Consejo Nacional de Ciencia y Technologia under Grant No. PCEXNA-040428.

[1]W. L. Mochán, M. del Castillo-Musot, and R. G. Barrera, Phys. Rev. B **35**, 1088 (1987).

[2]H. Köstlin, R. Jost, and W. Lems, Phys. Status Solidi A **29**, 87 (1975); I. Hanberg, C. G. Granqvist, K. F. Berggren, B. E. Sernelius, and L. Ergström, Vacuum **35**, 207 (1985); F. Demichelis, E. Minetti-Mezzeti, V. Smurro, A. Tagliaferro, and E. Tresso, J. Phys. D **18**, 1825 (1985).

[3]Z. A. Zheng, C. M. Falco, J. B. Ketterson and I. K. Schuller, Appl. Phys. Lett. **38**, 424 (1981); I. K. Schuller and C. M. Falco, Surf. Sci. **113**, 443 (1982).

[4]G. Eliasson, G. F. Giuliani, and J. J. Quinn, Phys. Rev. B **33**, 1405 (1986).

[5]Dengping Xue and Chien-hua Tsai, Solid State Commun. **56**, 651 (1985).

[6]F. Forstmann and H. Stenschke, Phys. Rev. B **17**, 1489 (1978); C. Schwartz and W. L. Schaich, J. Phys. **17**, 537 (1984).

[7]M. del Castillo-Mussot and W. L. Mochán, Solid State Commun. **62**, 556 (1987).

[8]R. E. Camley and D. L. Mills, Phys. Rev. B **29**, 1695 (1984); G. F. Giuliani, J. J. Quinn, and R. F. Wallis, J. Phys. (Paris) Colloq. **45**, C5-285 (1984).